Neuron, Vol. 42, 37–49, April 8, 2004, Copyright ©2004 by Cell Press

Critical Role of Ena/VASP Proteins for Filopodia Formation in Neurons and in Function Downstream of Netrin-1

Cecile Lebrand,[1,5] Erik W. Dent,[1,5] Geraldine A. Strasser,[1] Lorene M. Lanier,[2] Matthias Krause,[1] Tatyana M. Svitkina,[3] Gary G. Borisy,[4] and Frank B. Gertler[1,*]

[1]Department of Biology
Massachusetts Institute of Technology
Cambridge, Massachusetts 02139

[2]Department of Neuroscience
University of Minnesota
Minneapolis, Minnesota 55455

[3]Department of Biology
University of Pennsylvania
Philadelphia, Pennsylvania 19104

[4]Department of Cell and Molecular Biology
Northwestern University Medical School
Chicago, Illinois 60611

Summary

Ena/VASP proteins play important roles in axon outgrowth and guidance. Ena/VASP activity regulates the assembly and geometry of actin networks within fibroblast lamellipodia. In growth cones, Ena/VASP proteins are concentrated at filopodia tips, yet their role in growth cone responses to guidance signals has not been established. We found that Ena/VASP proteins play a pivotal role in formation and elongation of filopodia along neurite shafts and growth cone. Netrin-1-induced filopodia formation was dependent upon Ena/VASP function and directly correlated with Ena/VASP phosphorylation at a regulatory PKA site. Accordingly, Ena/VASP function was required for filopodial formation from the growth cone in response to global PKA activation. We propose that Ena/VASP proteins control filopodial dynamics in neurons by remodeling the actin network in response to guidance cues.

Introduction

During development, axons and dendrites are guided to their appropriate targets by growth cones. Growth cones must travel great distances and continually integrate a plethora of extracellular signals into appropriate changes in cytoskeletal dynamics to execute proper movement. During axonal outgrowth, growth cones extend numerous long filopodia, thin processes comprised of bundled actin filaments, that are thought to play a role both in sensing guidance cues and in facilitating locomotion (reviewed in Dickson, 2002). The elaboration of filopodia and the guided movement of growth cones require continuous and coordinated remodeling of the actin cytoskeleton (Dent and Gertler, 2003). One family of proteins implicated both in axon guidance and actin filament dynamics is the Ena/VASP protein family (Lanier et al., 1999).

Drosophila Enabled (Ena) was identified by its genetic interactions with the Abl tyrosine kinase (Gertler et al., 1990, 1995) and was later found to function in several signaling pathways essential for axon guidance in the developing nervous system (Lanier and Gertler, 2000). *Drosophila Ena* mutants exhibit CNS defects (Gertler et al., 1995) and a "bypass" phenotype in which ISNb nerve fails to branch at a defined point (Wills et al., 1999). Genetic analysis in *Drosophila* also reveals a role for Ena function downstream of the repulsive guidance receptor Robo (Bashaw et al., 2000). The *C. elegans* Ena homolog UNC-34 functions downstream of both UNC-40/DCC and UNC-5, Netrin-1 receptors that mediate attractive and repulsive responses, respectively (Colavita and Culotti, 1998; Gitai et al., 2003), as well as the *C. elegans* Robo ortholog Sax3 (Yu et al., 2002).

There are three related Ena/VASP proteins in vertebrates: Mena, EVL, and VASP (Gertler et al., 1996). In mice, deletion of Mena causes defects in the formation of the corpus callosum and the hippocampal commissure (Lanier et al., 1999). Specific neutralization of all Ena/VASP proteins in neurons migrating through the developing neocortex results in aberrant positioning of early-born pyramidal neurons in the superficial layers of the cortex, indicating that Ena/VASP proteins play a key role in regulating neuronal migration (Goh et al., 2002).

Ena/VASP family members are concentrated at the leading edges of protruding lamellipodia (Gertler et al., 1996; Reinhard et al., 1992; Rottner et al., 1999) and the tips of filopodia on growth cones (Lanier et al., 1999), sites where actin polymerization occurs (Forscher and Smith, 1988; Mallavarapu and Mitchison, 1999; Okabe and Hirokawa, 1991; Pollard and Borisy, 2003). Therefore, this protein family is perfectly positioned to be involved in early rearrangement of the actin cytoskeleton in response to a detected guidance cue. The three vertebrate Ena/VASP family members are highly related and can function interchangeably to support actin-dependent processes such as motility of the intracellular pathogen *Listeria monocytogenes* and regulation of lamellipodial dynamics (Geese et al., 2002; Laurent et al., 1999; Loureiro et al., 2002). Ena/VASP proteins contain specific domains that are shared in all family members (Bear et al., 2001; Gertler et al., 1996). These domains include the N-terminal EVH1 domain (for Ena/VASP homology) that plays a key role in subcellular targeting of Ena/VASP by binding specific proline-rich motifs found in a number of cellular proteins including Robo (Bashaw et al., 2000). In the middle of the protein is a proline-rich domain that binds SH3 and WW domain-containing proteins and the actin monomer binding protein profilin. The C-terminal EVH2 domain mediates tetramerization and binds both G and F actin (Bachmann et al., 1999; Huttelmaier et al., 1999). EVH2-mediated interactions with growing ends of actin filaments are required for Ena/VASP targeting to lamellipodia and filopodia (Bear et al., 2002).

*Correspondence: fgertler@mit.edu
[5]These authors contributed equally to this work.

Insight into the molecular mechanism of Ena/VASP function has come from a combination of cell biological and biochemical studies. Fibroblasts lacking functional Ena/VASP proteins display a hypermotile phenotype (Bear et al., 2000) that results from increased duration and stability of lamellipodial protrusions despite the fact that such Ena/VASP-deficient lamellipodia protrude much slower than controls (Bear et al., 2002). Over time, the behavior of slow but persistent protrusion is integrated into higher net rates of whole cell translocation. Lamellipodial protrusion in fibroblasts is driven by assembly of branched networks of actin filaments. Growth (monomer addition) occurs at actin filaments' barbed ends that are oriented toward the plasma membrane. In the absence of Ena/VASP proteins, actin networks are comprised of short, highly branched filaments. In contrast, excess Ena/VASP function leads to actin networks with longer, less branched filaments that produce rapidly protruding but short-lived lamellipodia. Biochemical experiments indicate that Ena/VASP proteins bind to growing actin filaments at or near their barbed ends and shield them from the activity of capping protein, which terminates filament elongation, making them "anticapping" proteins (Bear et al., 2002).

Function of the vertebrate Ena/VASP proteins is regulated by cyclic nucleotide-dependent kinases PKA and PKG (Reinhard et al., 2001). For example, VASP is required to mediate PKA-dependent attenuation of platelet activation (Aszodi et al., 1999; Hauser et al., 1999). Although they contain different numbers of PKA/PKG phosphorylation sites, Mena, EVL, and VASP all share one highly conserved PKA site located between the EVH1 domain and the polyproline-rich region. Mutation of the conserved site to a nonphosphorylatable alanine residue results in a protein that is properly localized but incapable of functioning to regulate fibroblast motility, while substitution of this residue with an aspartic acid residue to mimic phosphorylation results in a functionally active protein (Loureiro et al., 2002).

Interestingly, many axon guidance molecules can be either attractive or repulsive depending on the status of cyclic nucleotide signaling within growth cones (Song and Poo, 1999). The relative intracellular levels of cyclic adenosine monophosphate (cAMP) and cyclic guanosine monophosphate (cGMP) can control whether a specific guidance cue will act in an attractive or repellent manner (Hong et al., 2000; Nguyen-Ba-Charvet et al., 2001; Nishiyama et al., 2003; Polleux et al., 2000; Song et al., 1997). For example, when the ratio of cAMP to cGMP is at normal baseline levels, Netrin-1 and BDNF are attractive, while myelin-associated glycoprotein (MAG) is repulsive. However, if cAMP levels are lowered by either pharmacological means or by addition of laminin, Netrin-1, and BDNF become repulsive (Hopker et al., 1999; Song and Poo, 1999). Conversely, if cAMP levels are increased above baseline levels, MAG becomes attractive. However, little is known about the targets of PKA that might regulate the response of growth cones to guidance factors (Song and Poo, 2001).

In the current study, we explored the mechanism by which Ena/VASP proteins transform guidance information into growth cone responses. We show that Ena/VASP proteins are essential for normal formation and elongation of growth cone filopodia and play a key role in the morphological response to Netrin-1 signaling. Phosphorylation of Ena/VASP at its main regulatory site correlates with morphological responses to Netrin-1 and Ena/VASP proteins play an essential role in the growth cone response to global PKA activation. These results provide evidence that Ena/VASP proteins directly regulate filopodial dynamics in response to guidance cues and are regulated by the activation of second messenger pathways that control growth cone behavior.

Results

Ena/VASP Proteins Regulate Morphology of Growth Cones and Neurite Shafts

In vertebrates, all neurons examined to date express two or all three Ena/VASP proteins (Lanier et al., 1999). Since the highly related family members exhibit overlapping functions (Bear et al., 2000; Loureiro et al., 2002), we used a previously described strategy designed to neutralize or enhance the activity of all Ena/VASP proteins simultaneously. Briefly, we utilized the highly specific interaction of the EVH1 domain of Ena/VASP proteins with the ligand motif DFPPPPXDE (abbreviated FP4) to relocalize the protein within cells (Bear et al., 2000). Targeting GFP fused to oligomers of this motif to the mitochondrial surface in fibroblasts ("FP4-Mito") depletes all detectable Ena/VASP proteins from their normal location within cells and sequesters them on the mitochondrial surface. FP4-Mito expression in Rat2 fibroblasts induces a phenotype similar to that of fibroblast lines that lack detectable Ena/VASP proteins. Expression of FP4-Mito causes no additional phenotypes in Ena/VASP-deficient fibroblasts, suggesting that FP4-Mito-induced phenotypes result only from neutralization of Ena/VASP function. Mutation of the phenylalanine residue to an alanine (AP4) ablates the interaction with the EVH1 domain, permitting the use of AP4 motifs as a specificity control for FP4 effects. The results of these and other published experiments indicate that the FP4-Mito construct is a specific and effective method of blocking Ena/VASP function (Bear et al., 2000; Goh et al., 2002). When the relocalization strategy was modified to recruit endogenous Ena/VASP proteins to the plasma membrane by the addition of a "CAAX" motif from the C terminus of Ras, which directs proteins to the inner leaflet of the plasma membrane ("FP4-CAAX"), phenotypes equivalent to Ena/VASP overexpression were observed (Bear et al., 2000). As a specificity control for the FP4-CAAX construct, the FP4 motif was also replaced by an inactive AP4 motif (AP4-CAAX).

We first verified that the relocalization strategies were effective in cultured hippocampal neurons. The constructs were inserted into an adenoviral expression system for use in primary neurons. In wild-type (uninfected), AP4-Mito-, and AP4-CAAX-expressing neurons, Ena/VASP proteins were distributed throughout the growth cone and enriched at the tips of filopodia (Figures 1A–A″ and 1B–B″, data not shown). In neurons expressing the FP4-Mito construct, Mena, VASP, and EVL were depleted from sites of normal localization and colocalized with GFP signal on the mitochondrial surface (Figures 1C–1C″ and data not shown). As observed previously

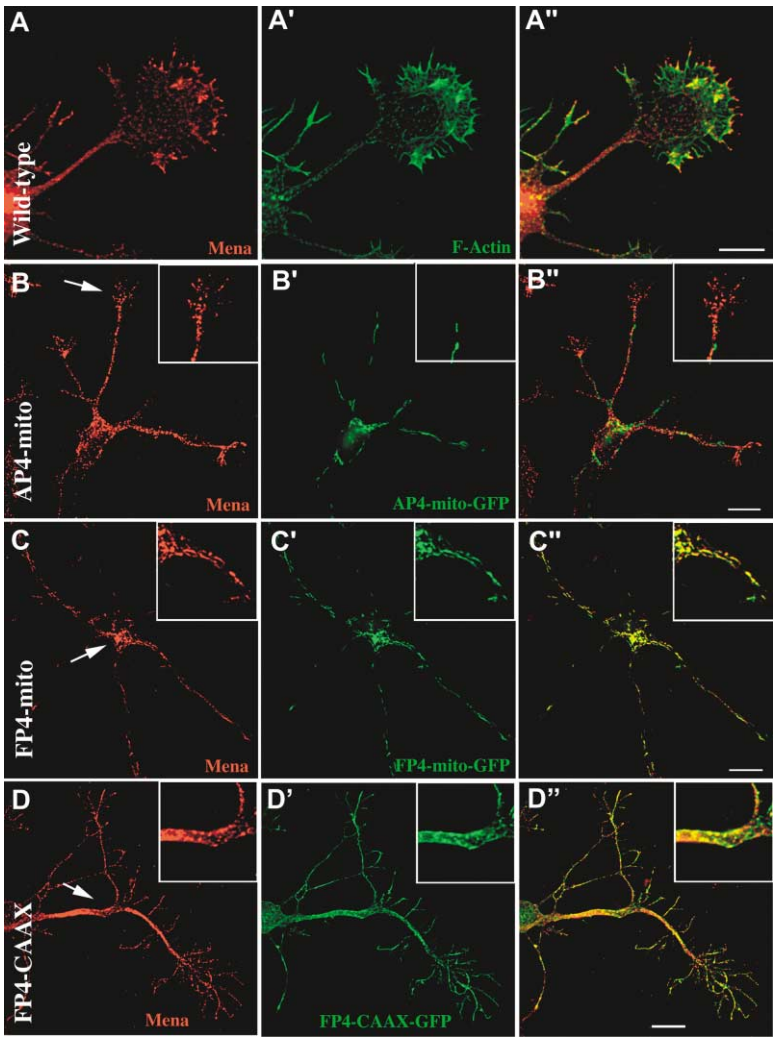

Figure 1. Expression of Mitochondria-Targeted and Plasma Membrane-targeted Ena/VASP Binding Proteins Sequester Ena/VASP Proteins

Wild-type hippocampal neurons (A–A″) and neurons expressing AP4-Mito-GFP (B–B″), FP4-Mito-GFP (C–C″), or FP4-CAAX-GFP (D–D″) were stained with an antibody to examine the distribution of Mena. Wild-type hippocampal neurons were also labeled with Oregon green-phalloidin (A′) to detect filamentous actin (F actin).

(A–A″) Mena (red) was enriched at the tips of growth cone filopodia, distal to F actin (green). As expected, neurons that expressed the AP4-Mito and the FP4-Mito constructs showed GFP-labeled mitochondria (B′ and C′, respectively).

(B–C″) Expression of the AP4-Mito construct (B–B″) did not displace Mena from its normal distribution, whereas expression of the FP4-Mito construct (C–C″) selectively depleted Mena from sites of normal localization and sequestered it on the mitochondrial surface.

(D–D″) Expression of FP4-CAAX construct increased Mena levels at the plasma membrane. At higher magnification, high levels of Mena at the plasma membrane clearly overlapped with spots of high expression levels of FP4-CAAX. Insets show magnified regions that are indicated by white arrows. Scale bar equals 10 μm.

in fibroblasts, expression of FP4-Mito did not result in the accumulation of F actin or a number of actin-associated proteins on the mitochondrial surface (data not shown). As expected, expression of the FP4-CAAX construct caused a redistribution of cytosolic Ena/VASP proteins to the plasma membrane (Figures 1D–1D″).

Primary hippocampal neurons expressing the relocalizing constructs were analyzed for morphology and behavior by time-lapse digital microscopy. As expected, both AP4-Mito- and AP4-CAAX-infected neurons exhibited behavior typical for wild-type hippocampal neurons, including lamellipodial dynamics and rapid filopodial extension, exploration, and withdrawal (Figures 2A, 2B, and 2D). In contrast, expression of FP4-Mito induced an apparent striking reduction in filopodia (Figure 2C). Quantification of fixed cells revealed a significant reduction in filopodia number along neurites shafts and growth cones in FP4-Mito-expressing neurons as compared to wild-type or AP4-Mito-expressing control neurons (Figure 3A). Furthermore, the few remaining filopodia on FP4-Mito neurites and growth cones were significantly shorter than controls (Figure 3A). Instead, FP4-Mito-expressing neurons frequently developed lamellipodia and ruffles (Figure 2C). Growth cone area in FP4-Mito-expressing neurons was increased 59% over AP4-Mito-expressing neurons (data not shown). Expression of FP4-CAAX induced a phenotype opposite to that observed with FP4-Mito (Figure 2E). FP4-CAAX-expressing neurons exhibited significant increases in the number and length of filopodia as compared to wild-type or AP4-CAAX-expressing neurons (Figure 3A). Filopodia in FP4-CAAX cells extended until they become unstable and retracted suddenly (Figure 2E). Extension of lamellipodial veils was restricted in FP4-CAAX-expressing cells. Therefore, in hippocampal neurons, neutralization of Ena/VASP causes reduction in the number and length of filopodia, while elevation of Ena/VASP activity has a reciprocal effect.

To quantify the role of Ena/VASP in neurite outgrowth and branching, neurons were fixed 2 days after plating and viral infection, stained with a tyrosinated tubulin antibody to label all neurites, and measured. Length of primary neurites, primary neurite number, and number of branches per cell was unaffected by AP4-Mito control construct expression. Neither the FP4-Mito nor the FP4-CAAX construct induced any statistically significant change in total neurite length per cell or in the length of the axon, which is the longest neurite (data not

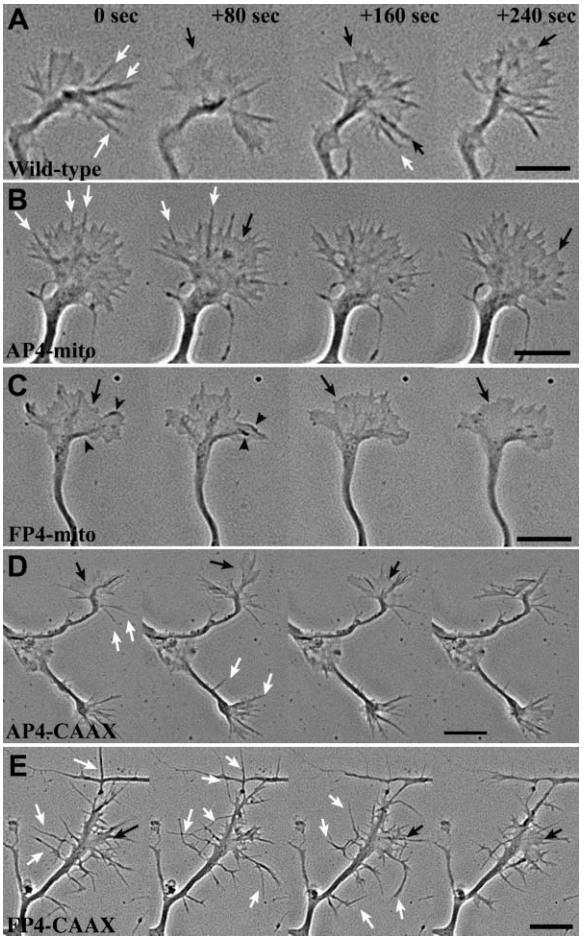

Figure 2. Relocalization of Ena/VASP Proteins Affects Growth Cone Dynamics

Phase time-lapse sequence of growth cone in wild-type neurons (A) and neurons expressing control AP4-Mito (B), FP4-Mito (C), control AP4-CAAX (D), and FP4-CAAX (E). Pictures illustrate growth cones at 80 s intervals. White arrows point to filopodia, black arrows to lamellipodia, and black arrowheads to lamellipodia ruffles.

(A) In wild-type neurons, growth cones are highly dynamic structures. Numerous filopodia and lamellipodia extended and retracted quickly at the surface of the growth cone.

(B and D) In control neurons infected with the AP4-Mito and the AP4-CAAX constructs, no major differences were observed. These neurons have highly motile filopodia and lamellipodia that could not be qualitatively differentiated from wild-type neurons.

(C) Growth cones of neurons expressing FP4-Mito nearly lost their capacity to generate filopodia and frequently developed lamellipodia and ruffles.

(E) FP4-CAAX-expressing neurons generated numerous extremely long filopodia at the growth cone and along the neurite. Scale bar equals 10 μm.

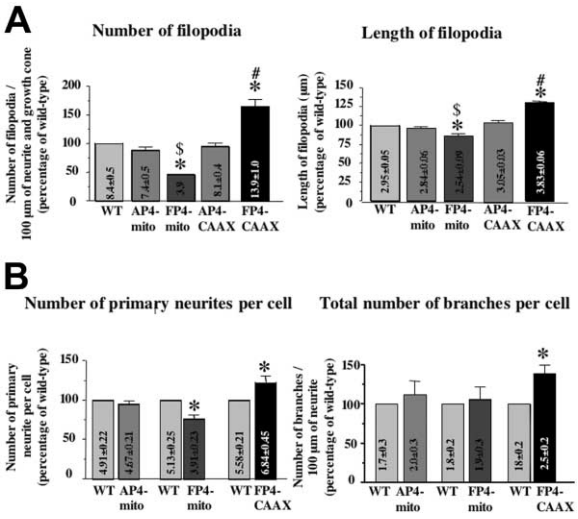

Figure 3. Ena/VASP Proteins Regulate Filopodia Formation and Branching

(A) Filopodia formation in wild-type neurons, and neurons expressing control AP4-Mito, FP4-Mito, control AP4-CAAX, or FP4-CAAX. Bars (mean ± SEM from samples of 25 neurons) represent the number of filopodia per 100 μm of neurite and growth cone ($n > 1000$ filopodia for each condition) and the length of filopodia expressed as a percentage of the values obtained for wild-type (noninfected) neurons. The actual means and SEMs are presented within the boxes. Expression of control AP4-Mito and AP4-CAAX constructs did not alter significantly the number or the length of filopodia in comparison to wild-type neurons. Expression of FP4-Mito decreased drastically the number of filopodia as compared to wild-type and control AP4-Mito, but the length of the remaining filopodia was only slightly reduced. Expression of FP4-CAAX increased significantly the number as well as the length of filopodia as compared to controls and to AP4-CAAX-expressing neurons.

(B) Branching in wild-type, control AP4-Mito, FP4-Mito, and FP4-CAAX-expressing neurons. Bars (means ± SEM from a sample of 50 neurons) represent the number of primary neurites per cell or the total number of branches per 100 μm neurite expressed as a percentage of the values in wt neurons observed on the same coverslip. In controls, expression of the AP4-Mito did not modify branching. Expression of FP4-Mito significantly reduced the number of primary neurites. Expression of FP4-CAAX resulted in a significant increase in the number of primary neurites and of the total number of branches per 100 μm of neurite. Data were collected from at least 3 separate experiments and compared by one-way ANOVA and Fisher's t tests.

*$p < 0.05$, compared with wild-type (noninfected) neurons. $$p < 0.05$, compared with the AP4-Mito control construct. #$p < 0.05$, compared with the AP4-CAAX control construct.

shown). The average length of individual neurite branch segments was also unaffected by FP4-Mito and FP4-CAAX. However, the number of primary neurites per cell was significantly decreased by FP4-Mito expression and increased by FP4-CAAX expression (Figure 3B). FP4-CAAX expression also increased the total number of branches per 100 μm of neurite. Therefore, despite the striking changes in growth cone morphology, expression of FP4-Mito or FP4 CAAX has no significant effect on net neurite outgrowth or the length of individual neurite branches, but does alter formation of primary neurites and branching throughout the neurite.

Effects of Ena/VASP Proteins on the Growth Cone Actin Cytoskeleton

Controls or neurons infected with FP4-Mito or FP4-CAAX were fixed and stained with phalloidin to examine the distribution of F actin within growth cones (Figure 4). Wild-type and AP4-Mito-expressing neurons exhibited characteristic thick bundles of F actin that extended from filopodia tips well into the peripheral region of the growth cone (Figures 4A and 4B). FP4-Mito-expressing neurons showed a dramatic reduction in bundled fila-

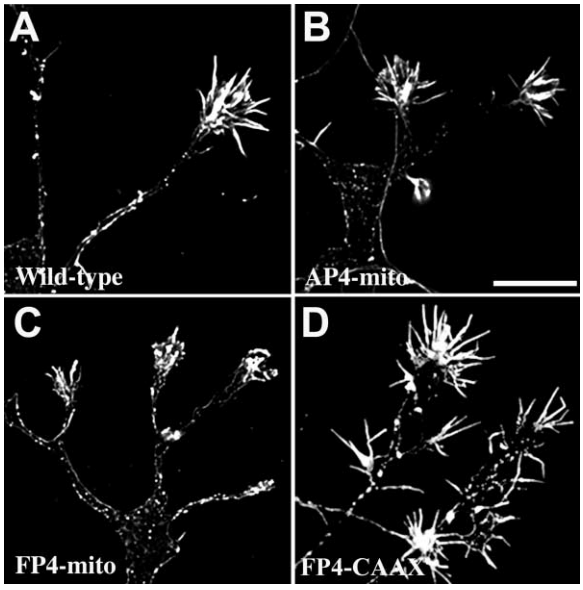

Figure 4. Ena/VASP Activity Controls Actin Cytoskeleton Organization

Effects of Ena/VASP on growth cone actin cytoskeleton in wild-type neurons and neurons expressing AP4-Mito, FP4-Mito, or FP4-CAAX constructs. Neurons were fixed and stained with phalloidin in order to examine the general distribution of actin filaments.

(A and B) In wild-type neurons as well as in AP4-Mito control neurons, actin labeling permitted the visualization of actin bundles in filopodia and in the palm of the growth cone.

(C) FP4-Mito-expressing neurons exhibit reduced numbers of actin filament bundles.

(D) Increased levels of Ena/VASP at the neuronal plasma membrane in FP4-CAAX-expressing neurons caused an increase in the number of actin filament bundles. Scale bar equals 20 μm.

ments, and instead frequently contained bands of F actin staining at the growth cone periphery (Figure 4C). In some cases, F actin staining was observed in patches in the central region of partially collapsed growth cones. In contrast, FP4-CAAX-expressing neurons exhibited a striking increase in the number of F actin bundles (Figure 4D). Similar changes were observed by staining with an antibody to ERM proteins, which decorates F actin bundles in the growth cone (not shown).

We examined the architecture of the cytoskeleton at higher resolution by EM analysis of platinum replicas of the actin cytoskeleton (Figure 5). As in earlier EM studies (Lewis and Bridgman, 1992), wild-type and control neurons contained thick bundles of filaments that underlie filopodia, while lamellipodial veils contained long filaments that appeared to be less branched or crosslinked than typical fibroblast lamellipodia (Figures 5A and 5B). Consistent with the results from fluorescence microscopy analysis, growth cones from FP4-Mito-expressing neurons exhibited a reduction or absence of the deep ribs of bundled actin filaments that comprise filopodia, an apparent reduction in long filaments as well as an increase in the density of networks of short actin filaments near the leading edge (Figure 5C). In contrast, FP4-CAAX-expressing neurons contained increased densities of long, thick, bundled actin filament ribs (Figure 5D). Therefore, the appearance of long, bundled F actin filaments and filopodia correlates with Ena/VASP levels.

Acute Netrin-1 Treatment Induces Lamellipodia and Filopodia Formation

Since genetic analysis in *C. elegans* implicates Ena/VASP function in Netrin-1-mediated guidance, we reasoned that changes in Ena/VASP levels might affect the response of cultured neurons to Netrin-1 application. We first analyzed the response of hippocampal neurons to bath application of Netrin-1. Using time-lapse digital microscopy, we observed that wild-type and control infected hippocampal neurons exhibited dramatic morphological changes within minutes of bath application of Netrin-1 (Figures 6A and 7A). Addition of either 50 or 600 ng/ml of Netrin-1 induced the formation of rapidly protruding and highly dynamic lamellipodia within 10–20 min, followed by the induction of filopodia on cell bodies, neurite shafts, and growth cones over the next 20–40 min (Figure 6A). While both Netrin-1 concentrations induced obvious morphological changes, the 600 ng/ml treatment induced more dramatic changes. Netrin-1-induced lamellipodia exhibited rapid cycles of protrusion and withdrawal. In addition, such lamellipodia frequently formed dynamic "waves" that traveled anterogradely and, less often, retrogradely along the neurite shaft. Quantification of the effects of 600 ng/ml Netrin-1 addition to hippocampal cultures showed that it increased the number and length of filopodia significantly between 40 and 60 min after addition (Figure 6D). The increase in filopodia length was still apparent when neurons were examined 18 hr after treatment (data not shown). We also quantified changes in lamellipodia number and area at various times after addition of 600 ng/ml Netrin-1. Lamellipodial number and area were significantly increased along the neurite shaft after 10 and 20 min of Netrin-1 addition, respectively (see Supplemental Figure S1 at http://www.neuron.org/cgi/content/full/42/1/37/DC1). In contrast, growth cone area was unchanged (not shown).

Netrin-1 is known to signal through the transmembrane receptor deleted in colorectal cancer (DCC) (Keino-Masu et al., 1996). To determine if the effects we observed were due to activation of DCC, we added a function-blocking antibody to DCC before and during Netrin-1 application. Addition of function-blocking DCC antibodies blocked the morphological response, confirming that DCC mediates the observed Netrin-1 effects (Figures 6B and 6D). Responses of neurons to Netrin-1 are also known to be influenced by levels of cAMP, which activate protein kinase A (PKA) (Ming et al., 2002; Nishiyama et al., 2003; Shewan et al., 2002). To determine if the Netrin-1-induced response was dependent upon PKA, we incubated neurons with a cocktail of PKA inhibitors (200 μM RP-cAMPs, 1 μM PKI, and 1 μM H89 or KT5720) for 1 hr before and during addition of 600 ng/ml Netrin-1. Blocking PKA activity abolished the effect of Netrin-1 (Figures 6C and 6D), indicating that the increase in filopodia length and number was dependent upon PKA activation. Incubation of neurons with either the DCC antibody or PKA inhibitor cocktail alone did not affect filopodia number and length (−5 and 0 time points in Figure 6D). Therefore, Netrin-1 treatment induces first

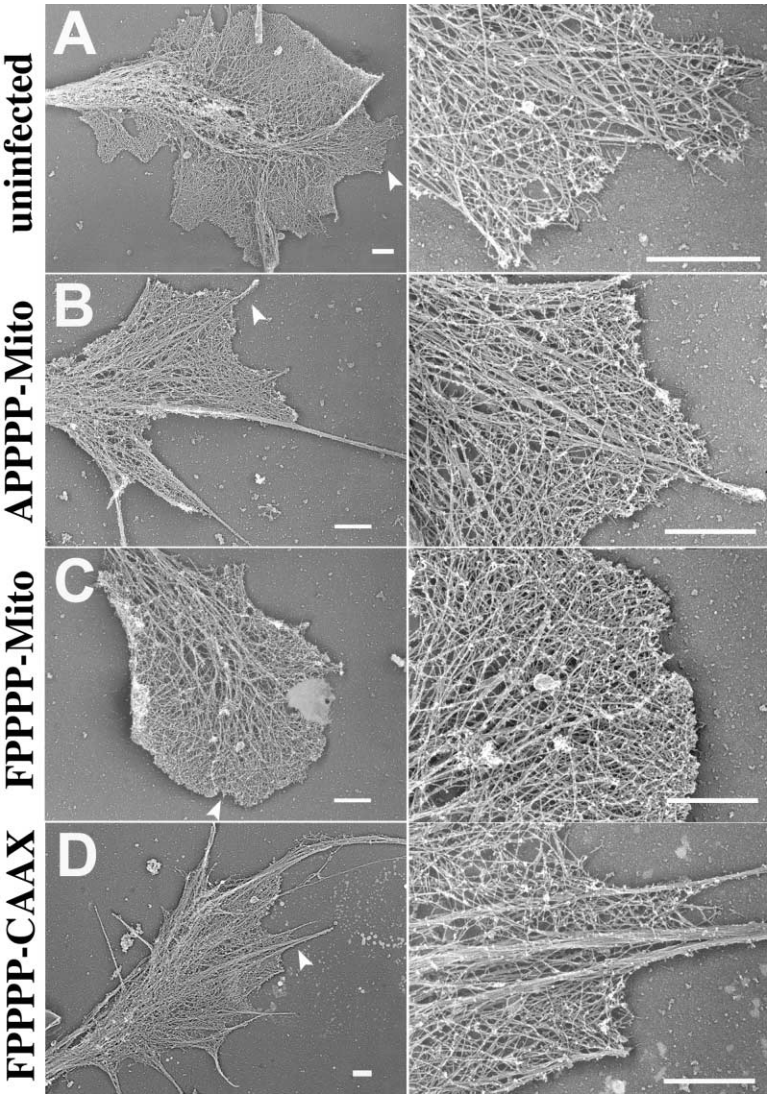

Figure 5. Ena/VASP Proteins Control Actin Filament Bundles

Platinum-replica TEM analysis of growth cones revealing the organization of the actin cytoskeleton. Arrowheads in the left column point to the area enlarged in the right column.
(A) In wild-type growth cones, numerous filopodia outlined by long parallel actin filaments (arrowheads) were alternating with a meshwork of actin filaments in the lamellipodia.
(B) Expression of AP4-Mito did not affect the organization of actin filaments (arrowheads) in the growth cone.
(C) Expression of FP4-Mito resulted in a loss of actin filament bundles (loss of filopodia) and a dense, randomly oriented actin meshwork in the peripheral growth cone.
(D) Expression of FP4-CAAX resulted in increased numbers of filopodia and actin bundles (arrowheads). Scale bars equal 0.1 μm.

lamellipodial, then filopodial protrusions along the axon shaft and growth cone by a mechanism dependent upon the DCC receptor and PKA activation.

Ena/VASP Is Required for Morphological Responses to Netrin-1

Neurons infected with the AP4-Mito, FP4-Mito, or FP4-CAAX constructs were treated with Netrin-1 and analyzed by time-lapse digital microscopy (Figures 7A–7C). As previously observed, FP4-Mito reduced the baseline numbers and lengths of filopodia on neurite shafts and growth cones, while FP4-CAAX increased both filopodial parameters. When normalized to these baselines, no significant changes in filopodial number or length were observed after Netrin-1 treatment in either the FP4-Mito or FP4-CAAX neurons (Figure 7D). Netrin-1 addition, however, still induced lamellipodial formation in both the FP4-Mito and FP4-CAAX cells (see Supplemental Figure S1 at http://www.neuron.org/cgi/content/full/42/1/37/DC1), indicating that this process can occur without Ena/VASP function. The resulting area of Netrin-1-induced lamellipodia was decreased in FP4-Mito expressing neurons, indicating that nascent lamellipodia either extended more slowly or ceased to extend earlier than in control neurons. These results indicate that neutralization or overactivation of Ena/VASP impairs the ability of neurons to initiate and elongate additional filopodia in response to Netrin-1 treatment.

Netrin-1 Induces Phosphorylation of Ena/VASP Proteins

Since signaling by Netrin-1 is dependent upon the levels of PKA activity within neurons (Nishiyama et al., 2003) and Ena/VASP proteins (Figure 7), we reasoned that Ena/VASP proteins might be phosphorylated by PKA in response to Netrin-1 treatment. To probe PKA phosphorylation of Mena, we developed an antibody specific to Mena when it is phosphorylated at serine 236 (Mena(s236)), the site conserved among all Ena/VASP family members. Addition of low concentrations of Netrin-1 (50 ng/ml) induced a rapid increase in phosphorylation of Mena that could be seen as early as 5 min after treatment (Figure 8A). Mena phosphorylation peaked at 30 min after treatment and was maintained at increased

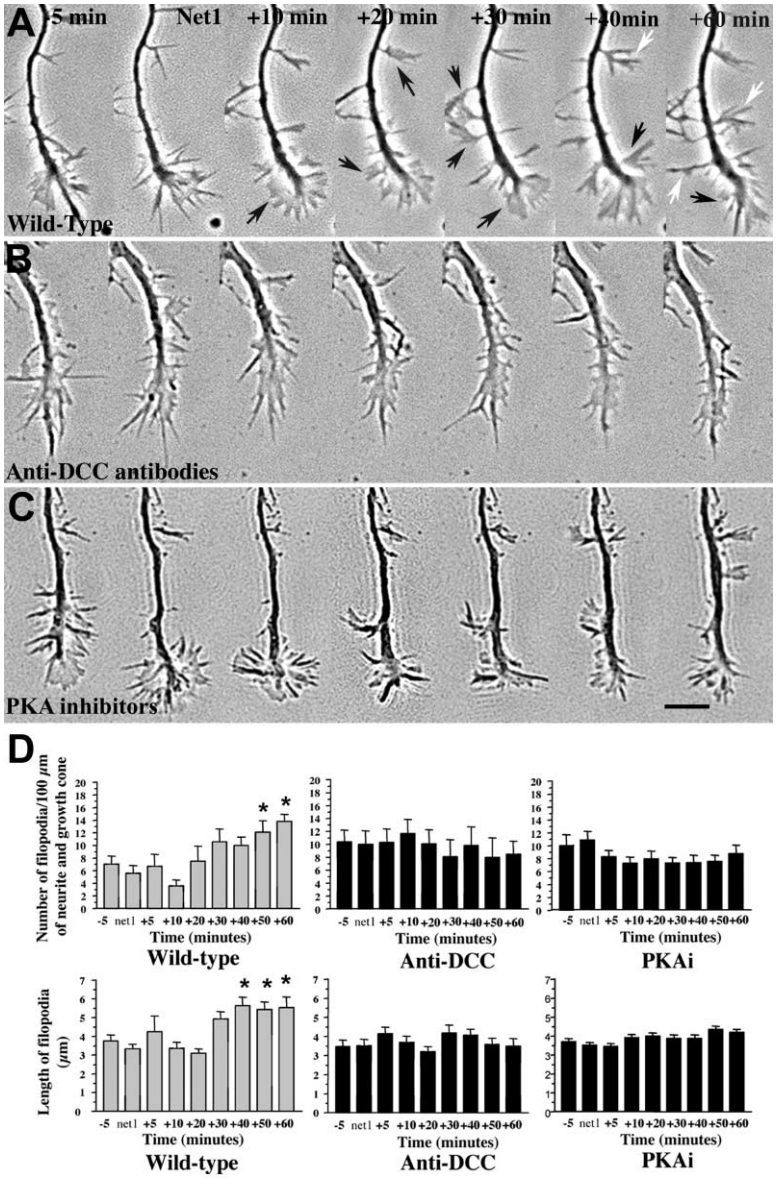

Figure 6. Netrin-1-Induced Filopodia Require DCC Receptor and PKA Activity

(A) Growth cones from wild-type neurons were imaged for 5 min before Netrin-1 addition and 60 min after addition. During the baseline period (illustrated 5 and 0 min prior to Netrin-1 application), no changes in lamellipodial and filopodial activities were observed. 10 min after Netrin-1 application, lamellipodia appeared along the neurite. Later, at 20–60 min after Netrin-1 application, filopodia protrusions appeared at multiple sites along the neurite shaft and growth cone. Black arrows point to lamellipodia, and white arrows point to filopodia.

(B) A growth cone from a wild-type neuron treated with 1.5 μg/ml of function-blocking anti-DCC receptor antibodies and imaged as in (A).

(C) A growth cone from a wild-type neuron treated with PKA inhibitors and imaged as in (A). Scale bar equals 10 μm.

(D) Netrin-1 (600 ng/ml) addition to wild-type neurons induced a marked increase in filopodia number and length over time (*$p < 0.05$ compared to time of Netrin-1 addition by repeated measures ANOVA). Bars (means ± SEM) represent the number ($n > 200$ filopodia for each time point) and the length of filopodia. Netrin-1 addition to wild-type neurons pretreated with either anti-DCC antibodies or PKA inhibitors (PKAi) increased neither the length nor the number of growth cone filopodia during the imaging period.

levels even after 2 hr (data not shown). These time points correlate with the induction of lamellipodial and filopodial protrusions induced by Netrin-1 addition (Figures 6 and 7). At high concentrations (600 ng/ml), Netrin-1 also induced an increase in phosphorylation of Mena but with a faster time course, peaking at about 5–10 min and decreasing to baseline by 1 hr after treatment (data not shown). Thus, the phosphorylation of Mena by Netrin-1 directly parallels the formation of filopodial protrusions after Netrin-1 treatment.

Ena/VASP Is Required for Morphological Responses to Global PKA Activation

Based on the correlation between Mena phosphorylation and the Netrin-1 response, we hypothesized that Ena/VASP proteins may be required for PKA-induced growth cone remodeling. To test this hypothesis, we first examined the effects of global activation of PKA by treatment of neurons with 20 μM forskolin, a potent activator of adenyl cyclase. Activation of adenyl cyclase increases the levels of cAMP, which activates protein kinase A (PKA). This treatment resulted in a dramatic phosphorylation of Mena after 30 min of treatment (Figure 8A). Interestingly, in wild-type neurons, forskolin induced a rapid increase in the number and length of filopodia, but not lamellipodia, in the growth cone (data not shown). However, unlike Netrin-1, forskolin had no effect on filopodial and lamellipodial dynamics along the axon shaft.

In addition to stimulating PKA activity, increased cAMP levels also activate the Rap1 guanine nucleotide exchange factor Epac (Stork, 2003). Addition of the specific Epac activator 8-pCPT-2′-O-Me-cAMP (Enserink et al., 2002), in the absense of forskolin, over a range of concentrations (25–100 μM), had no effect on the number or length of growth cone filopodia (data not shown), indicating that cAMP-dependent activation of Epac was not involved in the observed growth cone responses to

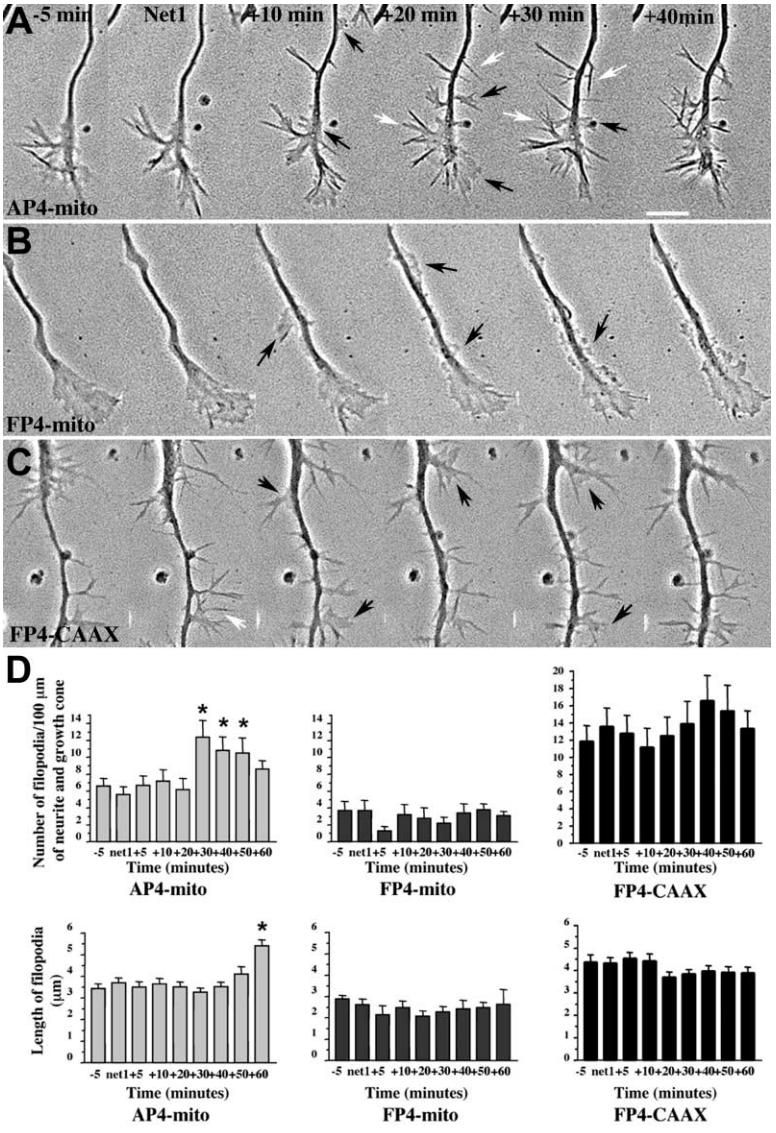

Figure 7. Netrin-1-Induced Filopodia Require Ena/VASP Activity

(A–C) Growth cone from control AP4-Mito-, FP4-Mito-, and FP4-CAAX-expressing neurons imaged for 5 min before and 40 min after Netrin-1 addition.

(A) In AP4-Mito-expressing neurons, during the baseline period (illustrated 5 and 0 min prior to Netrin-1 application), no changes in lamellipodial and filopodial activities were observed. 10 min after Netrin-1 application, lamellipodia appeared along the neurite. Later, at 20–30 min after Netrin-1 application, filopodia protrusions appeared at multiple sites along the neurite shaft and growth cone.

(B) Expression of the FP4-Mito construct completely blocked the increase of filopodia induced by Netrin-1.

(C) Expression of the FP4-CAAX construct increased the baseline number and length of filopodia and Netrin-1 application did not increase either of these parameters. White arrows point to filopodia extensions. Black arrows point to lamellipodia extensions. Scale bar in (A) corresponds to 10 μm in (A)–(C).

(D) Quantification of the filopodial responses to Netrin-1 in the three conditions. Bars (means ± SEM) represent the number ($n > 200$ filopodia for each time point) and the length of the filopodia. Netrin-1 induced a significant increase in number of filopodia in the control AP4-Mito between 30 and 50 min after Netrin-1 application. The increase in filopodia number was followed by a significant increase in their length at 60 min. No significant increase in number or length of filopodia was observed in FP4-Mito- or FP4-CAAX-expressing neurons. Data were collected from 3 separate experiments and compared by one-way or repeated ANOVA and Fisher's t tests. *$p < 0.05$, compared with baseline activity at 5 min and 0 min before Netrin-1 application.

forskolin. However, incubation of neurons with a cocktail of PKA inhibitors (200 μM Rp-cAMPs, 1 μM PKI, and 1 μM H89) significantly reduced the forskolin-induced effects on filopodia (data not shown). These data indicate that activation of PKA promotes filopodial formation and elongation in the growth cone.

To determine if Ena/VASP proteins were required for the forskolin-induced filopodial response, we infected neurons with either AP4-Mito, FP4-Mito, or FP4-CAAX followed by treatment with 20 μM forskolin, the same concentration found to induce marked phosphorylation of Mena (Figure 8A). AP4-Mito-expressing neurons exhibited a quantitative increase in the number and length of filopodial protrusions after forskolin treatment (Figures 8B and 8E), similar to that of uninfected neurons (data not shown). Interestingly, infection with FP4-Mito abolished the forskolin-induced increase in filopodial protrusions (Figures 8C and 8E). The few filopodia that were present on the growth cones of FP4-Mito-expressing neurons did not significantly increase in length after treatment with forskolin (Figures 8C and 8E). Nevertheless, FP4-Mito-expressing neurons did respond with lamellipodia ruffling, but did not significantly increase their growth cone area (data not shown). FP4-CAAX-infected neurons did not show an increase in filopodia number or length after 20 μM forskolin addition (Figures 8D and 8E), indicating that activation of Ena/VASP is likely to maximally stimulate the induction of growth cone filopodia in cultured hippocampal neurons.

Discussion

Ena/VASP Proteins Promote Filopodia Initiation, Elongation, and/or Stabilization in Neurons

Our current results demonstrate a direct correlation between the levels of Ena/VASP activity and the ability of neurons to form and extend filopodia. Inactivating Ena/VASP proteins markedly inhibited both normal and Netrin-1- or forskolin-induced filopodia formation in hippocampal neurons. We also demonstrate a positive corre-

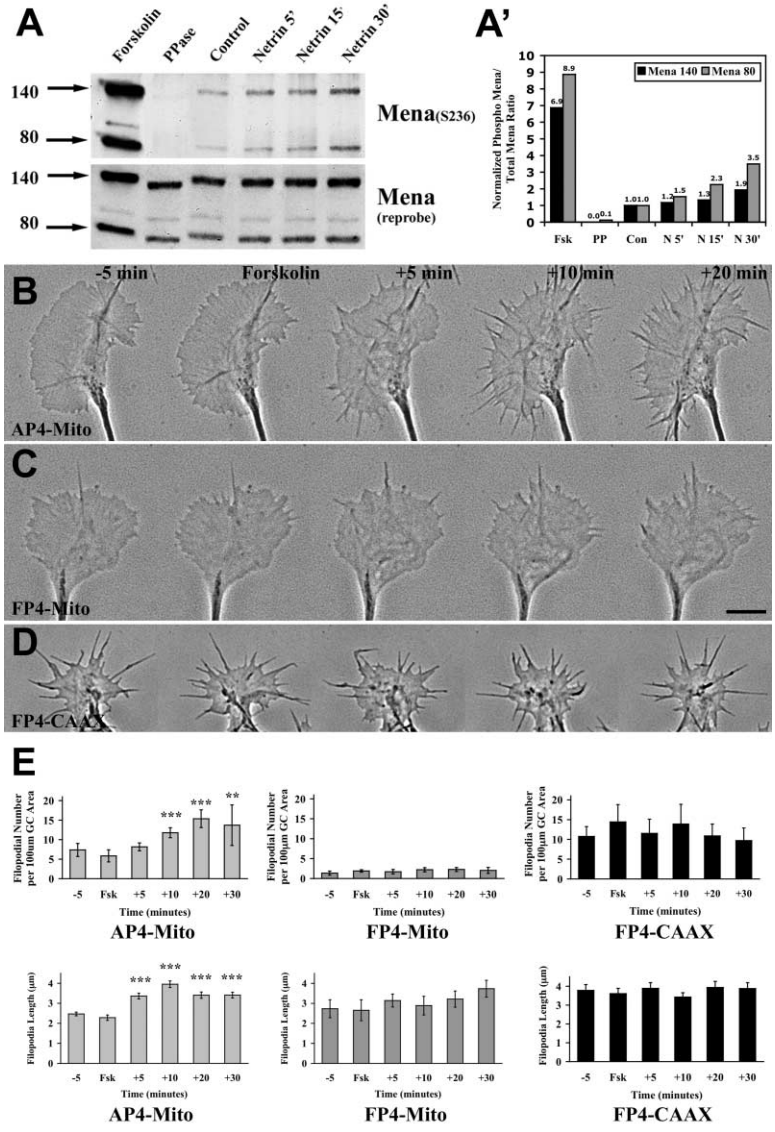

Figure 8. Forskolin-Induced Filopodia Require Ena/VASP Activity and Correlate with Mena Phosphorylation

(A) Western blot of cortical/hippocampal neurons after forskolin and Netrin-1 addition. Neurons were cultured for 36 hr and treated with 50 ng/ml Netrin-1 for varying times or 20 μM forskolin for 30 min. Phosphorylated Mena (Mena(S236)) was detected with a phosphospecific antibody. Note lack of staining in phosphatase (PPase)-treated samples. Blot was reprobed after complete stripping with a polyclonal Mena antibody that recognizes all forms of Mena to show equal loading of lanes. Arrows at 80 and 140 kd indicate the Mena and Mena^{+} isoforms.

(A′) Quantification of amount of phosphorylated Mena after forskolin and Netrin-1 treatments.

(B) Growth cone from a control AP4-Mito-expressing neuron imaged for 5 min before forskolin addition and 20 min after addition.

(C) Growth cone from an FP4-Mito-expressing neuron treated with forskolin and imaged as in (B). Scale bar equals 10 μm in (B)–(D).

(D) Growth cone from an FP4-CAAX-expressing neuron treated with forskolin and imaged as in (B) and (C).

(E) Forskolin addition to AP4-Mito-expressing neurons induced a marked increase in filopodia length and number over time (**$p < 0.01$, ***$p < 0.001$ compared to time of forskolin addition by repeated measures ANOVA). Bars (means ± SEM) represent the number ($n > 200$ filopodia for each time point) and the length of filopodia. Forskolin addition to FP4-Mito- and FP4-CAAX-expressing neurons increased neither the length nor the number of growth cone filopodia during the imaging period.

lation between Mena phosphorylation and these effects on filopodia.

The requirement for Ena/VASP function in neuronal filopodia formation fits well with a model for filopodia initiation proposed by Svitkina and colleagues (Svitkina et al., 2003). In this model, filament barbed ends within actin networks become "privileged" and escape the effects of capping proteins to elongate, become bundled, and form filopodia. The anticapping activity of Ena/VASP, as well as its ability to inhibit or reduce branching of actin filaments, suggest that Ena/VASP could play a role in the formation of the privileged filaments. Indeed, concentration of Ena/VASP is an early marker for nascent filopodia (Svitkina et al., 2003). Interestingly, *Dictyostelium* lacking their VASP ortholog exhibit reduced numbers of filopodia (Han et al., 2002).

In further support of this model for Ena/VASP function, during development, increased localization of *Drosophila* Ena at the apical cortex of epithelial cells correlates with increased persistence and elongation of filopodia-like microvilli (Grevengoed et al., 2003). Furthermore, in certain genetic backgrounds, the effects of reducing Ena levels are exactly opposite to the effects of reducing capping protein levels. Together, these data obtained using *Drosophila* genetics support a model in which Ena/VASP functions antagonistically to capping proteins in the formation and elongation of filopodia or filopodial-like structures.

Previous work in fibroblasts revealed an obvious link between Ena/VASP function and lamellipodial dynamics. In fibroblasts, Ena/VASP levels correlate positively with protrusion velocity and negatively with duration of the protrusion step. Because fibroblast translocation correlates more precisely with the persistence of lamellipodia protrusion, Ena/VASP proteins acted as negative regulators of fibroblast locomotion. Interestingly, alteration of Ena/VASP levels in neurons had no significant effect on neurite elongation, suggesting that there was no global effect on growth cone translocation.

Why do neurons and fibroblasts appear to respond

differently to alterations in Ena/VASP levels? It is likely that the effect of Ena/VASP function depends upon cellular context. Ena/VASP promotes actin filament elongation by antagonizing capping protein and also decreasing the density of actin filament branches. In fibroblasts, excess Ena/VASP activity gives rise to networks of long, sparsely branched individual actin filaments that are presumably too flexible to oppose the forces of membrane tension, thereby giving rise to rapid but unstable protrusions (Bear et al., 2002). In growth cones, the long, unbranched filament networks formed by Ena/VASP are bundled and therefore likely become stiff enough to form protrusive filopodia. In the absence of Ena/VASP function, growth cone lamellipodia are composed of a network of actin filaments that are shorter and appear similar to the branched actin networks typical of fibroblasts.

It seems likely that key differences between growth cones and fibroblasts would involve the concentration and distribution of branching and bundling proteins. The Arp2/3 complex plays a major role in controlling the geometry of actin networks in a variety of contexts including the lamellipodia of keratocytes and fibroblasts (Pollard and Borisy, 2003). Arp2/3 activity nucleates the formation of new actin filaments off the sides of existing filaments at a characteristic 70° angle. Arp2/3 is enriched at the periphery of lamellipodia in fibroblasts and keratocytes. In contrast, neuronal growth cones exhibit high concentrations of Arp2/3 in their central domains and in neurite shafts but lack detectable Arp2/3 enrichment at their periphery (G. Strasser et al., submitted). It is possible that relatively lower levels of Arp2/3-branching/nucleating activity in the growth cone periphery produce a synergistic effect with Ena/VASP to favor filopodia formation.

Role of Ena/VASP Function in Axon Guidance

We propose that Ena/VASP proteins play a key role in growth cone pathfinding by regulating the formation and dynamics of growth cone filopodia, structures that are critical for interpreting guidance information. Filopodia are known to concentrate and extend on the side of the growth cone facing an attractive gradient of guidance cues (Zheng et al., 1996). Conversely, disruption of growth cone filopodia with actin depolymerization agents, both in culture and in vivo, cause growth cone disorientation (Bentley and Toroian-Raymond, 1986; Chien et al., 1993; O'Connor et al., 1990). Growth cone filopodia are thought to generate mechanical force by pulling against the underlying substratum (Suter and Forscher, 2000) and to transduce distal signals through calcium fluctuations and calpain activation (Davenport and Kater, 1992; Robles et al., 2003; Song and Poo, 1999). Thus, filopodia have been ascribed both mechanical and sensory roles in neurite outgrowth and guidance (Dickson, 2002). The guidance defects observed in *Drosophila Ena* mutants and in Mena knockout mice (Gertler et al., 1995; Lanier et al., 1999; Wills et al., 1999) may in part arise from a compromised ability of neurons to form or elongate filopodia.

Ena/VASP was required for the morphological response of neurons to Netrin-1. Acute Netrin-1 treatment induced an Ena/VASP-independent increase in the number of lamellipodia protrusions, followed by an Ena/VASP-dependent increase of filopodia protrusion and elongation. The Netrin-1 effects we observed required DCC, a receptor that mediates growth cone turning and promotes neurite outgrowth (de la Torre et al., 1997; Forcet et al., 2002; Metin et al., 1997; Serafini et al., 1996). Furthermore, the Netrin-1-induced increase in filopodia number and elongation was dependent upon PKA activity. Given that Mena phosphorylation by PKA correlated with the response to Netrin-1, it is possible that mammalian Ena/VASP proteins are targets of a signaling cascade downstream of Netrin-1/DCC. This is consistent with genetic data in *C. elegans* indicating that UNC-34, an Ena/VASP homolog, functions downstream of the UNC-40/DCC receptor (Gitai et al., 2003).

Genetic studies have also demonstrated a role for Ena/VASP proteins in response to repulsive guidance cues (Bashaw et al., 2000; Colavita and Culotti, 1998; Yu et al., 2002), leading to the speculation that Ena/VASP might act by suppressing growth cone translocation, similar to the way in which Ena/VASP negatively regulates fibroblast motility. Our data, however, indicate that neutralization or elevation of Ena/VASP function had no significant effect on overall neurite elongation, but significantly altered filopodia formation.

We propose that the primary role of Ena/VASP in growth cones is to regulate filopodia dynamics. Given that filopodia are remodeled in response to both attractive and repulsive guidance signals in vitro (Song and Poo, 1999; Zheng et al., 1996) and the fact that growth cones become larger and have more filopodia when they pause at guidance choice points in vivo (Dingwell et al., 2000; Mason and Wang, 1997), it is possible that Ena/VASP-regulated filopodial activity may mediate responses to both attractive and repulsive signals. In such a model, the function of Ena/VASP proteins in attraction and repulsion would depend upon the differential distribution and/or activation of Ena/VASP across the growth cone. A repulsive cue may preferentially reduce Ena/VASP activity on the side of the growth cone closest to the repulsive cue. This would cause a loss of bundled actin and reduced filopodial dynamics and result in turning away from the repulsive cue. Conversely, an attractive cue may activate Ena/VASP proteins only in the filopodia facing the source of guidance factor.

How is Ena/VASP activity regulated during guidance? It is known that the intracellular levels of cyclic adenosine monophosphate (cAMP) and cyclic guanosine monophosphate (cGMP) can control whether a specific guidance cue acts in an attractive or repulsive manner (Song and Poo, 1999). Vertebrate Ena/VASP proteins are phosphorylated by PKA, as well as PKG, and the phosphorylation is required for full function in a number of cellular contexts (Kwiatkowski et al., 2003; Reinhard et al., 2001). Phosphorylation is known to affect electrophoretic mobility of Ena/VASP proteins, suggesting that phosphorylation could induce a conformational change in the molecule. Phosphorylation also modulates Ena/VASP's interactions with some binding partners. Further work will be required, however, to determine how phosphorylation induces Ena/VASP to remodel the actin network. We have shown that Mena is phosphorylated at a key regulatory PKA site upon Netrin-1 treatment and that Ena/VASP proteins are required for the increase in

growth cone filopodia induced by either Netrin-1 or PKA activation. Localized guidance cues might induce gradients of Ena/VASP phosphorylation across the growth cone, resulting in the selective extension and stabilization of filopodia in response to guidance cues.

Experimental Procedures

Plasmids

Subcloning and PCR were performed using standard methods. The FP4-Mito, AP4-Mito, FP4-CAAX, and AP4-CAAX constructs were prepared as previously described (Bear et al., 2000). Recombinant adenoviruses capable of expressing these constructs and EGFP were generated and purified as previously described (He et al., 1998). Primary hippocampal neurons were infected at a multiplicity of infection of 100 pfu/cell with various controls (AP4-Mito, AP4-CAAX, GFP) or FP4-Mito- and FP4-CAAX-expressing adenoviruses. They survived and appeared healthy at least 3 days after infection for low to medium levels of GFP expression. Having verified that all the effects of the control constructs were equivalent, the AP4-Mito construct was used in the majority of the experiments as a control of potential toxicity due to virus infection and GFP overexpression.

Antibodies and Reagents

The polyclonal anti-Mena (2197), anti-VASP (2010), and anti-EVL (1404) antibodies were generated in the laboratory and previously described (Bear et al., 2000; Lanier et al., 1999). The 13H9 monoclonal antibody against radixin (ERM protein) was a generous gift of Dr. Frank Solomon. The following antibodies were purchased from the indicated companies: monoclonal antibodies against human DCC (Ab-1) from Oncogene (San Diego, CA); monoclonal antibodies against βIII tubulin from Promega (Madison, WI); and monoclonal antibodies against rat anti-tyrosinated tubulin from Chemicon International (Temecula, CA). Labeled secondary antibodies were purchased from Jackson ImmunoResearch Laboratories (West Grove, PA). Alexa 594, Alexa 647, and Oregon green phalloidin were from Molecular Probes (Eugene, OR), recombinant chicken Netrin-1 was from R&D systems (Minneapolis, MN), cytochalasin D and forskolin were from Sigma (St. Louis, MO), λ-phosphatase was from New England Biolabs (Beverly, MA), 8-pCPT-2′-O-Me-cAMP was from Biolog/Axxora (San Diego, CA), and RP-cAMPs, PKI 14-22 amide, H-89, and KT5720 were from Calbiochem.

Production of monoclonal anti-Mena antibody was accomplished as follows. His-tagged full length Mena + and a fragment of Mena + comprising only the + exon were produced in insect cells using the "Bac-to-Bac" baculovirus expression system according to the protocols supplied by the manufacturer (GIBCO-BRL) and purified on cobalt beads (BD Talon resins, BD Biosciences Clontech). These recombinant proteins were used to produce monoclonal antibodies in Mena$^{-/-}$ mice as described (Niebuhr et al., 1998). Hybridoma supernatants were screened by ELISA on recombinant, purified Mena + and the + exon of Mena, on Western blots of extracts of adult mouse brain, and in immunofluorescence microscopy of MV D7 cells expressing GFP-Mena^{+}. One hybridoma was chosen and subcloned twice. By subclass analysis, this monoclonal antibody designated A351F7D9 was identified as IgG2b.

Production of the phosphospecific polyclonal antibody to the conserved PKA site on Mena (S236) was accomplished as follows. The immunogen peptide NH2-WERERRMSNAAPSSD (S = phosphoserine) was used to produce polyclonal antibodies, and the antibodies were affinity purified on a phospho peptide column.

Cell Culture, Immunocytochemistry, and Imaging of Fixed Cells

Primary hippocampal neurons were prepared from E16 mouse as described for E18 rat (Goslin and Banker, 1989). Glial cultures were prepared from P1 mouse cortex and hippocampus as described (Voutsinos-Porche et al., 2003). Hippocampal neurons were plated on poly-D-lysine-coated coverslips and maintained in glial-conditioned medium (Neurobasal, 2% B27, 1% Glutamine [GIBCO-BRL]). After 24–48 hr, cells were fixed in 4% paraformaldehyde/PBS, blocked with 10% BSA/PBS, and permeabilized with 0.2% triton/PBS. Coverslips were incubated with primary antibody for 45 min follow by secondary antibody for 45 min. For detection of F actin, labeled phalloidin was added to the secondary antibody solution. Coverslips were mounted in Mowiol and were analyzed with a Zeiss Axiophot fluorescence microscope equipped with 20× or 40× Plan-NEOFLUAR objectives or 63× Plan-NEOFLUAR oil immersion objectives. Coverslips were imaged using a Deltavision deconvolution system (Applied Precision).

Acute Effects of Netrin-1 and Forskolin on the Morphology of Neurons

For imaging experiments, neurons were plated onto nitric acid-cleaned, poly-D-lysine-coated Assistent German glass coverslips (Carolina Biologicals). These coverslips were previously attached to 35 mm plastic culture dishes (Corning) in which holes 15 mm in diameter had been machine drilled (Dent and Kalil, 2003). In these sets of experiments, neurons were grown in unconditioned medium because cultures grown in glial-conditioned medium produced too much variability upon guidance factor/drug treatment. After 24–36 hr in culture, chambers were opened and placed on the stage of a Nikon TE300 microscope. Temperature was maintained at 37°C and CO_2 was maintained at 5% with the aid of a microscope incubator system (Solent Scientific Limited, UK). Selected neurons were imaged with a 40×/0.95NA Plan Apo objective at 20 s intervals. Images were captured with an Orca-ER cooled CCD camera (Hammamatsu, Japan). All peripherals were controlled with Openlab software (Improvision). Pictures were processed in Adobe Photoshop or Metamorph (Universal Imaging) and converted into Quicktime movies with OpenLab.

Only infected neurons expressing low levels of GFP were chosen for imaging. Netrin-1 or forskolin were added directly to the culture dish while imaging. In some Netrin-1 experiments, anti-DCC antibodies (1.5 μg/ml) were added to cultures 1 hr before treatment with Netrin-1. Changes in growth cone size, lamellipodia number/area, and filopodia number/length were measured manually with the aid of Openlab software. At least 5 neurons per treatment from 3 separate experiments were analyzed by one-way or repeated measures ANOVA and Fisher's t tests.

Analysis of Morphological Differences in Fixed Cultures

We fixed cultures at various time points and analyzed them by immunofluorescence with a variety of probes for actin (phalloidin, radixin) and microtubules (βIII-, acetylated, or tyrosinated α-tubulin). Filopodia parameters were determined by measuring filopodia number and length after labeling fixed cultures with phalloidin to highlight the filopodia. Filopodia number and size were quantified on images taken with a 63×/1.4NA Plan Apo objective using Deltavision software. The extent of neuronal outgrowth was determined by measuring neurite length and branching after labeling fixed cultures with antibodies to tyrosinated tubulin to highlight the neurites. The following parameters were evaluated: total neurite length, length of the longest neurite (axon), length of each branch segment, number of primary neurites per cell, and total number of branches per 100 μm of neurite. All measurements were performed on pictures taken with a 20× objective using Neurolucida software. More than 50 neurons per treatment from 3 separate experiments were analyzed by one-way ANOVA and Fisher's t tests.

Platinum Replica Electron Microscopy

Correlative platinum replica electron microscopy was performed essentially as described (Svitkina and Borisy, 1998) with a few minor modifications. Briefly, dissociated embryonic hippocampal neurons were cultured as described above on coverslips coated with a gold locator grid. EGFP-positive cells were located by live cell fluorescence microscopy and then immediately extracted for 3–5 min with 1% Triton X-100 in PEM buffer containing 2 mM phalloidin, 0.2% gluteraldehyde, and 4.2% sucrose as an osmotic buffer. Coverslips were washed with PEM and fixed with 2% gluteraldehyde in 0.1 M Na-cacodylate (pH 7.3) and processed for electron microscopy. Cells previously identified as EGFP-positive were relocated using the gold grid for micrographs.

Immunoprecipitation and Western Blotting

Neocortex and hippocampal cortex were dissected out of E16 mice and treated as above except they were plated at 5–10 $\times$ 10^6 cells/60 cm dish. Neurons were cultured for 36 hr and treated with 50 ng/ml Netrin-1 for varying times or 20 μM forskolin for 30 min. Cultures were solubilized in 400 μl ice cold extraction buffer (1% IGEPAL CA-630, 150 mM NaCl, 50 mM TRIS [pH 8.0], 15 mM sodium pyrophosphate, 50 mM sodium fluoride, 40 mM β-glycerophosphate, 1 mM sodium vanadate [all Sigma], and Complete protease inhibitor cocktail tablet [Roche]). Solubilized and unsolubilized material was centrifuged at 14,000 rpm for 5 min at 4°C. Supernatants were removed for immunoprecipitation. One control culture was treated with λ-phosphatase (NEB) according to manufacturer's directions. Supernatants were immunoprecipitated with a mouse monoclonal antibody to Mena (see antibody production section) and protein A sepharose (Pierce). After extensive washing, bound protein was solubilized in sample buffer and run on 8% polyacrylamide gels. Gels were transferred overnight to Immobilon (Millipore) and probed with an affinity-purified (see antibody production section) rabbit polyclonal antibody to the PKA phosphorylation site in Mena (1:500) and an HRP-coupled donkey anti-rabbit secondary (1:10,000) (Jackson Immunologicals). Blots were developed in ECL+ (Amersham-Pharmacia).

Acknowledgments

This project was initiated and most of the reagents were generated by L.M.L. We thank members of the Gertler lab for helpful discussion and comments on the manuscript. C.L. was a recipient of a fellowship from the EMBO. F.B.G. was supported by a W.M. Keck Distinguished Young Scholar award. This work was supported by NIH grants NS45366 to E.W.D. and GM62431 to G.G.B and by a Cell Migration Consortium grant U54 GM64346 to G.G.B and GM68678 to F.B.G.

Received: September 16, 2003
Revised: December 23, 2003
Accepted: February 5, 2004
Published: April 7, 2004

References

Aszodi, A., Pfeifer, A., Ahmad, M., Glauner, M., Zhou, X.H., Ny, L., Andersson, K.E., Kehrel, B., Offermanns, S., and Fassler, R. (1999). The vasodilator-stimulated phosphoprotein (VASP) is involved in cGMP- and cAMP-mediated inhibition of agonist-induced platelet aggregation, but is dispensable for smooth muscle function. EMBO J. *18*, 37–48.

Bachmann, C., Fischer, L., Walter, U., and Reinhard, M. (1999). The EVH2 domain of the vasodilator-stimulated phosphoprotein mediates tetramerization, F-actin binding, and actin bundle formation. J. Biol. Chem. *274*, 23549–23557.

Bashaw, G.J., Kidd, T., Murray, D., Pawson, T., and Goodman, C.S. (2000). Repulsive axon guidance: Abelson and Enabled play opposing roles downstream of the roundabout receptor. Cell *101*, 703–715.

Bear, J.E., Loureiro, J.J., Libova, I., Fassler, R., Wehland, J., and Gertler, F.B. (2000). Negative regulation of fibroblast motility by Ena/VASP proteins. Cell *101*, 717–728.

Bear, J.E., Krause, M., and Gertler, F.B. (2001). Regulating cellular actin assembly. Curr. Opin. Cell Biol. *13*, 158–166.

Bear, J.E., Svitkina, T.M., Krause, M., Schafer, D.A., Loureiro, J.J., Strasser, G.A., Maly, I.V., Chaga, O.Y., Cooper, J.A., Borisy, G.G., and Gertler, F.B. (2002). Antagonism between Ena/VASP proteins and actin filament capping regulates fibroblast motility. Cell *109*, 509–521.

Bentley, D., and Toroian-Raymond, A. (1986). Disoriented pathfinding by pioneer neurone growth cones deprived of filopodia by cytochalasin treatment. Nature *323*, 712–715.

Chien, C.B., Rosenthal, D.E., Harris, W.A., and Holt, C.E. (1993). Navigational errors made by growth cones without filopodia in the embryonic *Xenopus* brain. Neuron *11*, 237–251.

Colavita, A., and Culotti, J.G. (1998). Suppressors of ectopic UNC-5 growth cone steering identify eight genes involved in axon guidance in *Caenorhabditis elegans*. Dev. Biol. *194*, 72–85.

Davenport, R.W., and Kater, S.B. (1992). Local increases in intracellular calcium elicit local filopodial responses in *Helisoma* neuronal growth cones. Neuron *9*, 405–416.

de la Torre, J.R., Hopker, V.H., Ming, G.L., Poo, M.M., Tessier-Lavigne, M., Hemmati-Brivanlou, A., and Holt, C.E. (1997). Turning of retinal growth cones in a netrin-1 gradient mediated by the netrin receptor DCC. Neuron *19*, 1211–1224.

Dent, E.W., and Gertler, F.B. (2003). Cytoskeletal dynamics and transport in growth cone motility and axon guidance. Neuron *40*, 209–227.

Dent, E.W., and Kalil, K. (2003). Dynamic imaging of neuronal cytoskeleton. Methods Enzymol. *361*, 390–407.

Dickson, B.J. (2002). Molecular mechanisms of axon guidance. Science *298*, 1959–1964.

Dingwell, K.S., Holt, C.E., and Harris, W.A. (2000). The multiple decisions made by growth cones of RGCs as they navigate from the retina to the tectum in *Xenopus* embryos. J. Neurobiol. *44*, 246–259.

Enserink, J.M., Christensen, A.E., de Rooij, J., van Triest, M., Schwede, F., Genieser, H.G., Doskeland, S.O., Blank, J.L., and Bos, J.L. (2002). A novel Epac-specific cAMP analogue demonstrates independent regulation of Rap1 and ERK. Nat. Cell Biol. *4*, 901–906.

Forcet, C., Stein, E., Pays, L., Corset, V., Llambi, F., Tessier-Lavigne, M., and Mehlen, P. (2002). Netrin-1-mediated axon outgrowth requires deleted in colorectal cancer-dependent MAPK activation. Nature *417*, 443–447.

Forscher, P., and Smith, S.J. (1988). Actions of cytochalasins on the organization of actin filaments and microtubules in a neuronal growth cone. J. Cell Biol. *107*, 1505–1516.

Geese, M., Loureiro, J.J., Bear, J.E., Wehland, J., Gertler, F.B., and Sechi, A.S. (2002). Contribution of Ena/VASP proteins to intracellular motility of listeria requires phosphorylation and proline-rich core but not F-actin binding or multimerization. Mol. Biol. Cell *13*, 2383–2396.

Gertler, F.B., Doctor, J.S., and Hoffmann, F.M. (1990). Genetic suppression of mutations in the *Drosophila* abl proto-oncogene homolog. Science *248*, 857–860.

Gertler, F.B., Comer, A.R., Juang, J.L., Ahern, S.M., Clark, M.J., Liebl, E.C., and Hoffmann, F.M. (1995). enabled, a dosage-sensitive suppressor of mutations in the *Drosophila* Abl tyrosine kinase, encodes an Abl substrate with SH3 domain-binding properties. Genes Dev. *9*, 521–533.

Gertler, F.B., Niebuhr, K., Reinhard, M., Wehland, J., and Soriano, P. (1996). Mena, a relative of VASP and *Drosophila* Enabled, is implicated in the control of microfilament dynamics. Cell *87*, 227–239.

Gitai, Z., Yu, T.W., Lundquist, E.A., Tessier-Lavigne, M., and Bargmann, C.I. (2003). The netrin receptor UNC-40/DCC stimulates axon attraction and outgrowth through enabled and, in parallel, Rac and UNC-115/AbLIM. Neuron *37*, 53–65.

Goh, K.L., Cai, L., Cepko, C.L., and Gertler, F.B. (2002). Ena/VASP proteins regulate cortical neuronal positioning. Curr. Biol. *12*, 565–569.

Goslin, K., and Banker, G. (1989). Experimental observations on the development of polarity by hippocampal neurons in culture. J. Cell Biol. *108*, 1507–1516.

Grevengoed, E.E., Fox, D.T., Gates, J., and Peifer, M. (2003). Balancing different types of actin polymerization at distinct sites: roles for Abelson kinase and Enabled. J. Cell Biol. *163*, 1267–1279.

Han, Y.H., Chung, C.Y., Wessels, D., Stephens, S., Titus, M.A., Soll, D.R., and Firtel, R.A. (2002). Requirement of a vasodilator-stimulated phosphoprotein family member for cell adhesion, the formation of filopodia, and chemotaxis in dictyostelium. J. Biol. Chem. *277*, 49877–49887.

Hauser, W., Knobeloch, K.P., Eigenthaler, M., Gambaryan, S., Krenn, V., Geiger, J., Glazova, M., Rohde, E., Horak, I., Walter, U., and Zimmer, M. (1999). Megakaryocyte hyperplasia and enhanced agonist-induced platelet activation in vasodilator-stimulated phosphoprotein knockout mice. Proc. Natl. Acad. Sci. USA *96*, 8120–8125.

He, T.C., Zhou, S., da Costa, L.T., Yu, J., Kinzler, K.W., and Vogelstein, B. (1998). A simplified system for generating recombinant adenoviruses. Proc. Natl. Acad. Sci. USA *95*, 2509–2514.

Hong, K., Nishiyama, M., Henley, J., Tessier-Lavigne, M., and Poo, M. (2000). Calcium signalling in the guidance of nerve growth by netrin-1. Nature *403*, 93–98.

Hopker, V.H., Shewan, D., Tessier-Lavigne, M., Poo, M., and Holt, C. (1999). Growth-cone attraction to netrin-1 is converted to repulsion by laminin-1. Nature *401*, 69–73.

Huttelmaier, S., Harbeck, B., Steffens, O., Messerschmidt, T., Illenberger, S., and Jockusch, B.M. (1999). Characterization of the actin binding properties of the vasodilator-stimulated phosphoprotein VASP. FEBS Lett. *451*, 68–74.

Keino-Masu, K., Masu, M., Hinck, L., Leonardo, E.D., Chan, S.S., Culotti, J.G., and Tessier-Lavigne, M. (1996). Deleted in Colorectal Cancer (DCC) encodes a netrin receptor. Cell *87*, 175–185.

Kwiatkowski, A.V., Gertler, F.B., and Loureiro, J.J. (2003). Function and regulation of Ena/VASP proteins. Trends Cell Biol. *13*, 386–392.

Lanier, L.M., and Gertler, F.B. (2000). From Abl to actin: Abl tyrosine kinase and associated proteins in growth cone motility. Curr. Opin. Neurobiol. *10*, 80–87.

Lanier, L.M., Gates, M.A., Witke, W., Menzies, A.S., Wehman, A.M., Macklis, J.D., Kwiatkowski, D., Soriano, P., and Gertler, F.B. (1999). Mena is required for neurulation and commissure formation. Neuron *22*, 313–325.

Laurent, V., Loisel, T.P., Harbeck, B., Wehman, A., Grobe, L., Jockusch, B.M., Wehland, J., Gertler, F.B., and Carlier, M.F. (1999). Role of proteins of the Ena/VASP family in actin-based motility of *Listeria monocytogenes*. J. Cell Biol. *144*, 1245–1258.

Lewis, A.K., and Bridgman, P.C. (1992). Nerve growth cone lamellipodia contain two populations of actin filaments that differ in organization and polarity. J. Cell Biol. *119*, 1219–1243.

Loureiro, J.J., Rubinson, D.A., Bear, J.E., Baltus, G.A., Kwiatkowski, A.V., and Gertler, F.B. (2002). Critical roles of phosphorylation and actin binding motifs, but not the central proline-rich region, for Ena/vasodilator-stimulated phosphoprotein (VASP) function during cell migration. Mol. Biol. Cell *13*, 2533–2546.

Mallavarapu, A., and Mitchison, T. (1999). Regulated actin cytoskeleton assembly at filopodium tips controls their extension and retraction. J. Cell Biol. *146*, 1097–1106.

Mason, C.A., and Wang, L.C. (1997). Growth cone form is behavior-specific and, consequently, position-specific along the retinal axon pathway. J. Neurosci. *17*, 1086–1100.

Metin, C., Deleglise, D., Serafini, T., Kennedy, T.E., and Tessier-Lavigne, M. (1997). A role for netrin-1 in the guidance of cortical efferents. Development *124*, 5063–5074.

Ming, G.L., Wong, S.T., Henley, J., Yuan, X.B., Song, H.J., Spitzer, N.C., and Poo, M.M. (2002). Adaptation in the chemotactic guidance of nerve growth cones. Nature *417*, 411–418.

Nguyen-Ba-Charvet, K.T., Brose, K., Marillat, V., Sotelo, C., Tessier-Lavigne, M., and Chedotal, A. (2001). Sensory axon response to substrate-bound Slit2 is modulated by laminin and cyclic GMP. Mol. Cell. Neurosci. *17*, 1048–1058.

Niebuhr, K., Lingnau, A., Frank, R., and Wehland, J. (1998). Rapid procedures for preparing monoclonal antibodies and identifying their epitopes. In Cell Biology: A Laboratory Handbook, second edition, volume 2, J.E. Celis, ed. (San Diego, CA: Academic Press), pp. 398–403.

Nishiyama, M., Hoshino, A., Tsai, L., Henley, J.R., Goshima, Y., Tessier-Lavigne, M., Poo, M.M., and Hong, K. (2003). Cyclic AMP/GMP-dependent modulation of Ca^{2+} channels sets the polarity of nerve growth-cone turning. Nature *424*, 990–995.

O'Connor, T.P., Duerr, J.S., and Bentley, D. (1990). Pioneer growth cone steering decisions mediated by single filopodial contacts in situ. J. Neurosci. *10*, 3935–3946.

Okabe, S., and Hirokawa, N. (1991). Actin dynamics in growth cones. J. Neurosci. *11*, 1918–1929.

Pollard, T.D., and Borisy, G.G. (2003). Cellular motility driven by assembly and disassembly of actin filaments. Cell *112*, 453–465.

Polleux, F., Morrow, T., and Ghosh, A. (2000). Semaphorin 3A is a chemoattractant for cortical apical dendrites. Nature *404*, 567–573.

Reinhard, M., Halbrugge, M., Scheer, U., Wiegand, C., Jockusch, B.M., and Walter, U. (1992). The 46/50 kDa phosphoprotein VASP purified from human platelets is a novel protein associated with actin filaments and focal contacts. EMBO J. *11*, 2063–2070.

Reinhard, M., Jarchau, T., and Walter, U. (2001). Actin-based motility: stop and go with Ena/VASP proteins. Trends Biochem. Sci. *26*, 243–249.

Robles, E., Huttenlocher, A., and Gomez, T.M. (2003). Filopodial calcium transients regulate growth cone motility and guidance through local activation of calpain. Neuron *38*, 597–609.

Rottner, K., Behrendt, B., Small, J.V., and Wehland, J. (1999). VASP dynamics during lamellipodia protrusion. Nat. Cell Biol. *1*, 321–322.

Serafini, T., Colamarino, S.A., Leonardo, E.D., Wang, H., Beddington, R., Skarnes, W.C., and Tessier-Lavigne, M. (1996). Netrin-1 is required for commissural axon guidance in the developing vertebrate nervous system. Cell *87*, 1001–1014.

Shewan, D., Dwivedy, A., Anderson, R., and Holt, C.E. (2002). Age-related changes underlie switch in netrin-1 responsiveness as growth cones advance along visual pathway. Nat. Neurosci. *5*, 955–962.

Song, H.J., and Poo, M.M. (1999). Signal transduction underlying growth cone guidance by diffusible factors. Curr. Opin. Neurobiol. *9*, 355–363.

Song, H., and Poo, M. (2001). The cell biology of neuronal navigation. Nat. Cell Biol. *3*, E81–E88.

Song, H.J., Ming, G.L., and Poo, M.M. (1997). cAMP-induced switching in turning direction of nerve growth cones. Nature *388*, 275–279.

Stork, P.J. (2003). Does Rap1 deserve a bad Rap? Trends Biochem. Sci. *28*, 267–275.

Suter, D.M., and Forscher, P. (2000). Substrate-cytoskeletal coupling as a mechanism for the regulation of growth cone motility and guidance. J. Neurobiol. *44*, 97–113.

Svitkina, T.M., and Borisy, G.G. (1998). Correlative light and electron microscopy of the cytoskeleton of cultured cells. Methods Enzymol. *298*, 570–592.

Svitkina, T.M., Bulanova, E.A., Chaga, O.Y., Vignjevic, D.M., Kojima, S., Vasiliev, J.M., and Borisy, G.G. (2003). Mechanism of filopodia initiation by reorganization of a dendritic network. J. Cell Biol. *160*, 409–421.

Voutsinos-Porche, B., Bonvento, G., Tanaka, K., Steiner, P., Welker, E., Chatton, J.Y., Magistretti, P.J., and Pellerin, L. (2003). Glial glutamate transporters mediate a functional metabolic crosstalk between neurons and astrocytes in the mouse developing cortex. Neuron *37*, 275–286.

Wills, Z., Bateman, J., Korey, C.A., Comer, A., and Van Vactor, D. (1999). The tyrosine kinase Abl and its substrate enabled collaborate with the receptor phosphatase Dlar to control motor axon guidance. Neuron *22*, 301–312.

Yu, T.W., Hao, J.C., Lim, W., Tessier-Lavigne, M., and Bargmann, C.I. (2002). Shared receptors in axon guidance: SAX-3/Robo signals via UNC-34/Enabled and a Netrin-independent UNC-40/DCC function. Nat. Neurosci. *5*, 1147–1154.

Zheng, J.Q., Wan, J.J., and Poo, M.M. (1996). Essential role of filopodia in chemotropic turning of nerve growth cone induced by a glutamate gradient. J. Neurosci. *16*, 1140–1149.